Bayesian Analysis Users Guide
Release 4.00, Manual Version 1

G. Larry Bretthorst
Biomedical MR Laboratory
Washington University School Of Medicine,
Campus Box 8227
Room 2313, East Bldg.,
4525 Scott Ave.
St. Louis MO 63110
http://bayes.wustl.edu
Email: larry@bayes.wustl.edu

October 21, 2016

Contents

List of Figures

List of Tables

Chapter 22

Phasing An Image

MRI Images present special problems for most data processing algorithms because of the use of the absolute value after the k-space data are Fourier transformed. When the absolute value is taken, the noise and the signal get multiplied. Unless the signal-to-noise in the data is very high, this cross-term can cause big problems in processing the data. However, this problem is eliminated if an absorption mode image is used because then the Fourier transform is a linear operator and if the noise was Gaussian in k-space, it remains Gaussian in the image domain. An example of an absorption mode image is shown in Fig. 22.1 as the left panel. The right panel is the same image in absolute value mode. Note that in the absorption model image, outside the brain the noise oscillates around zero and close inspection of the images will revel that the absorption mode image is sharper than the absolute value image. The effect is not as pronounced in images as it is in spectroscopic applications because the echos do not decay appreciably in the time needed to acquire them. Nonetheless sharper images and eliminating the noise offsets are two very strong reasons to use absorption mode images. In this Chapter we describe the Bayesian calculations needed to create an absorption mode images.

The image phasing package, Bayes Phase, estimates three phase parameters. These phase parameters may be estimated from one image and then applied to all images in an array, they may be determined for each image separately, or they may be determined for one image. In the all cases the output from the package is a series of FDF and Ascii files that may then be displayed in Vnmr, VnmrJ or they may be viewed using image browser. Additionally, these output phased images may be used to generate input data for other packages, and they my be analyzed in total to generate images of various parameter maps that are output from these other packages. For example, after a set of images have been phased individual voxel intensities may be imported into the diffusion tensor analysis and then analyzed. Or the images could be input to the Image Pixel package and then an image of the diffusion constants could be generated.

The calculations presented in this Chapter describe the imaging model and then present three separate Bayesian calculations: one for the constant phase, and then two identical calculations for the positionally dependent phase shift in each of the two spatial domains. The program that implements this calculation can processes spin echo, gradient echo and EPI images. In the case of EPI images four phase parameters are needed to phase an image, in the directly detected domain an even and odd time delay are needed, additionally, one time delay is needed in the indirectly detected domain and finally one constant phase is needed. The calculations for these four phase parameters are exactly identical to the calculations for the spin echo and gradient echo phase parameters and

Figure 22.1: Absorption Model Images

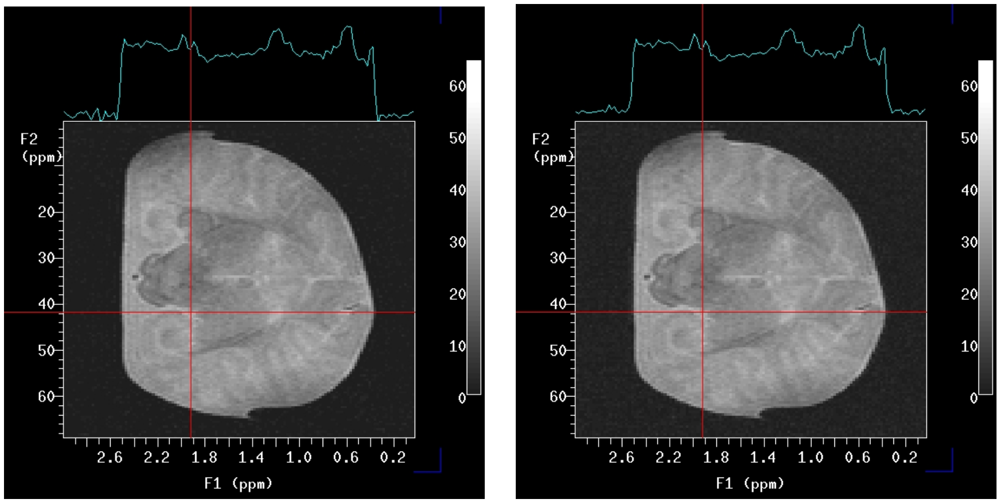

Figure 22.1: The left panel is an example of an absorption mode image while the right panel is the same image in absolute value. A single trace has been displayed on both images. Note that in the absorption image outside the brain the noise oscillates around zero and the image comes down faster on the brain boundary.

we will not have much more to say about EPI images except to note how to analyze them.

The Bayes Phase package is accessed by selecting the "Phase An Image" button on the dispatching menu. When this button is activated the interface window shown in Fig. 22.2 is displayed. The upper panel in this figure is the heart of the VnmrJ interface while the lower panel is the Vnmr interface. Both interfaces set a number of control parameters and then allow one to run the phasing algorithm.

22.1 The Bayesian Calculation

There are three phase parameters that must be determined to produce an absorption mode image: a constant phase θ, and two time delays which we will designate as τ_x and τ_y. These time delays may also be thought of as the center of the echo in the k-space, and they are analogous to the frequency dependent phase in spectroscopic measurements. In spectroscopic application, frequency dependent phase shifts are typically small. Indeed it is rare to find spectroscopic data that have frequency dependent shifts that cause more than one or two phase wraps. However, in imaging τ_x and τ_y are huge and typically cause 180° phase wraps every few points in the Fourier transform. Indeed these phase wraps are so big, that in the image domain the data look as if it has a periodic signal in it, as indeed it does.

To estimate these three phase parameters, one must relate these parameters to the data through a model. If we expand the spin density in sinc functions in the spatial domain, then in the k-space

Figure 22.2: The Interface To The Image Phasing Package

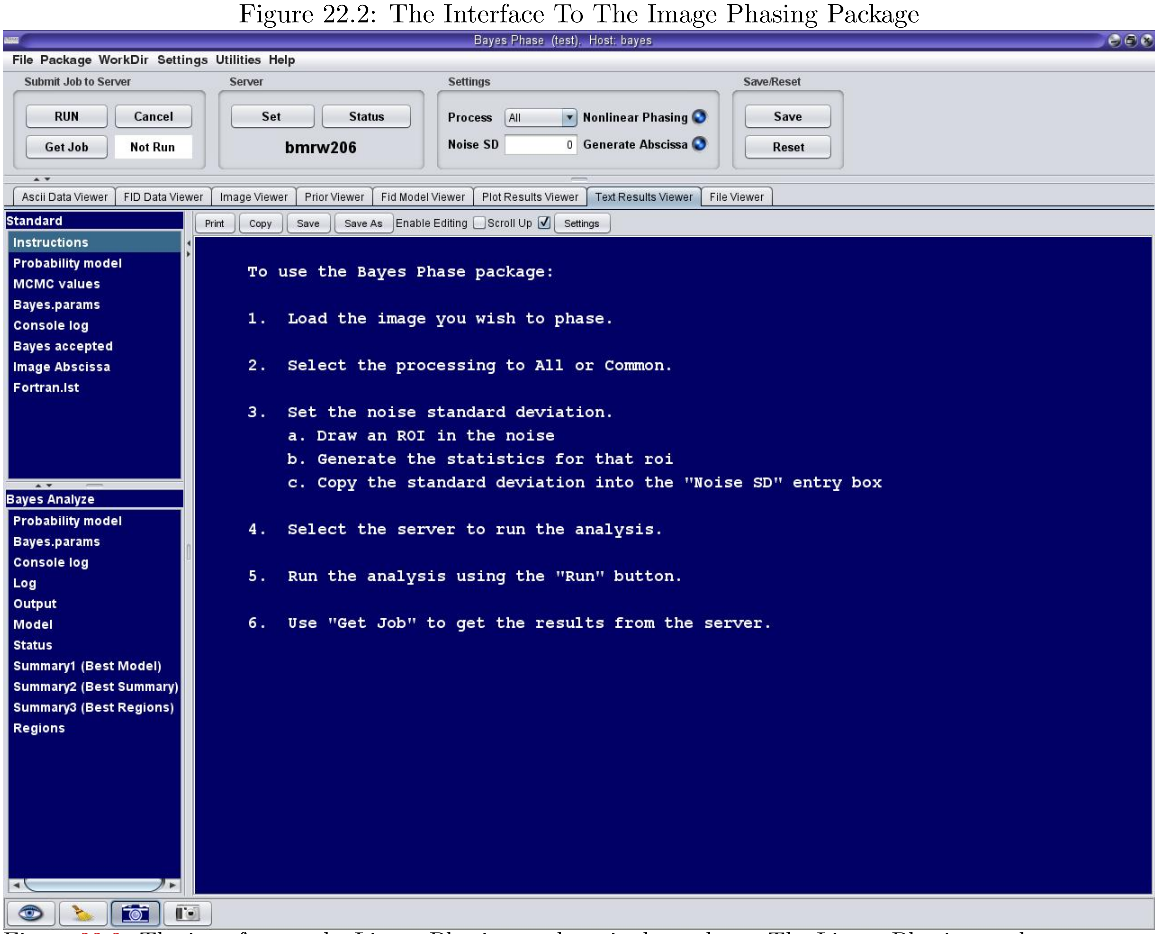

Figure 22.2: The interface to the Linear Phasing package is shown here. The Linear Phasing package outputs a series of FDF files that contain the real and imaginary parts of the phased images. These images may then be used as input to other packages. For example the are often used by the Analyze Image Pixel package.

domain the expansion is a Fourier series:

$$d_{ij} = \exp\{-\mathrm{i}\theta\} \sum_{k=1}^{N_x} \sum_{l=1}^{N_y} A_{kl} \exp\{-2\pi\mathrm{i}(x_k(t_{xi} + \tau_x) - 2\pi\mathrm{i}(y_l(t_{yj} + \tau_y)\} + \text{noise} \tag{22.1}$$

where we have designated the complex data as d_{ij}, N_x and N_y are the number of complex data values in the x and y domains, and the intensity of the spin density function at position x_k and y_l has been designated as A_{kl}. We have intentionally written this model in a way that explicitly shows that the two sums over the k-space data are time shifted inverse Fourier transforms. Note that as written the phase parameters τ_x and τ_y do participate in the sums. However the Bayesian calculations are time domain calculations, and in these calculations the sums will be over i and j and we will find that τ_x and τ_y do not participate in the sums. As a result, the Bayesian calculations may be done using fast discrete Fourier transform when N_x and N_y are powers of 2.

We will start this process by estimating τ_x. If we are only interested in τ_x, the value of both τ_y and θ are irrelevant to us. For the purposes of estimating τ_x we note that the imaging experiment just increments the value of y by a constant for each k-space acquisition. Effectively this just changes the constant phase of each new k-space acquisition. Consequently, for the purposes of estimating τ_x we will rewrite Eq. (22.1) as

$$d_{ij} = \exp\{-\mathrm{i}\theta_j\} \sum_{k=1}^{N_x} B_{kj} \exp\{-2\pi\mathrm{i}(x_k(t_{xi} + \tau_x)\} + \text{noise} \tag{22.2}$$

where B_{kj} are the amplitudes of the image in the jth k-space acquisition. Similarly, the phase θ_j is the constant phase in the jth k-space acquisition. Both of these quantities are related to the A_{kl} and θ through a complicated sum. Fortunately, we don't care about these expressions for estimating τ_x. Separating this model into its real and imaginary parts one has

$$d_{Rij} = \sum_{k=1}^{N_x} B_{kj} M_{Rki} + \text{noise} \tag{22.3}$$

for the real data, and

$$d_{Iij} = \sum_{k=1}^{N_x} -B_{kj} M_{Iki} + \text{noise} \tag{22.4}$$

for the quadrature data where

$$M_{Rki} \equiv \cos(\theta)\cos(2\pi x_k[t_{xi} + \tau_x]) + \sin(\theta)\sin(2\pi x_k[t_{xi} + \tau_x]) \tag{22.5}$$

and

$$M_{Iki} \equiv \cos(\theta)\sin(2\pi x_k[t_{xi} + \tau_x]) - \sin(\theta)\cos(2\pi x_k[t_{xi} + \tau_x]). \tag{22.6}$$

In this model the data may be thought of as N_y different data sets each of them bearing on the value of τ_x. If each data set contributes independent information about τ_x, then the posterior probability will just be the product of the probabilities for τ_x in each data set separately. Consequently, the marginal posterior probability for τ_x can be factored to obtain

$$P(\tau_x|DI) = \int d\sigma \prod_{j=1}^{N_y} \int dB_{1j} \ldots dB_{N_x j} d\theta_j P(B_{1j} \ldots B_{N_x j} \theta_j \sigma | D_j I) \tag{22.7}$$

where D_j is just the data for the jth k-space acquisition.

The right-hand side of this equation is factored using Bayes' theorem to obtain:

$$P(\tau_x|DI) \propto \int d\sigma \prod_{j=1}^{N_y} \int dB_{1j} \ldots dB_{N_xj} d\theta_j P(B_{1j} \ldots B_{N_xj}\theta_j\sigma|I) P(D_j|B_{1j} \ldots B_{N_xj}\theta_j\sigma I). \quad (22.8)$$

Finally, the joint prior probability for the parameters is factored using the product rule to obtain

$$\begin{aligned} P(\tau_x|DI) \quad \propto \quad & \int d\sigma P(\sigma|I) \prod_{j=1}^{N_y} \int dB_{1j} \ldots dB_{N_xj} d\theta_j \\ \times \quad & P(\theta_j|I) P(B_{1j} \ldots B_{N_xj}|I) P(D_j|B_{1j} \ldots B_{N_xj}\theta_j\sigma I) \end{aligned} \quad (22.9)$$

where we have not factored the prior probability for the amplitudes, $P(B_{1j} \ldots B_{N_xj}|I)$, into independent prior probabilities because we are going to assign a correlated prior to the amplitudes. That is to say we are going to take into account the fact that images tend to be smoothly varying and that adjacent voxels tend to be very nearly equal.

We have now reached the point in the Bayesian calculation where one has no choice but to assign a numerical value to represent each of these probabilities. The prior probability for the noise standard deviation, $P(\sigma|I)$, will be assigned a Jeffreys' prior

$$P(\sigma|I) \propto \frac{1}{\sigma}. \quad (22.10)$$

The prior probability for the phase, $P(\theta_j|I)$, will be assigned a uniform prior probability and this prior will restrict the integration over the phase to zero to 2π.

In assigning the prior probability for the amplitudes we wish to take into account the fact that adjacent amplitudes tend to be nearly equal. Of coarse there are always exceptions to this, but nonetheless, in this analysis we are going to put in a prior that will try and make adjacent voxels equal. Here is how this is done. If $B_{kj} \approx B_{k+1j}$ then

$$B_{kj} \approx B_{k+1j} \Rightarrow B_{kj} - B_{k+1j} \approx 0 \Rightarrow \sum_{k=1}^{N_x-1} (B_{kj} - B_{k+1j})^2 \text{ is small.} \quad (22.11)$$

If the principle of Maximum Entropy is used to assign a prior probability that imposes this condition, Maximum Entropy will lead to a Gaussian assignment for the prior. This Gaussian will be written as

$$P(B_{1j} \ldots B_{N_xj}|I) \propto \left(\frac{\sigma}{\beta}\right)^{-N_x} |U_{kl}|^{-\frac{1}{2}} \exp\left\{-\sum_{k=1}^{N_x}\sum_{l=1}^{N_x} \frac{B_{lj}\beta^2 U_{kl} B_{kj}}{2\sigma^2}\right\} \quad (22.12)$$

where the matrix U_{kl} is a tri-diagonal matrix having [-1, 2,-1] as its three non-zero diagonals and β expresses how strongly we believe adjacent voxels should be equal. In the program that implements this calculation $\beta = 0.1$, so the prior says that we think small oscillations, on the order of 0.01 of the maximum signal value are probably noise. Note we are using this condition only in the calculation of τ_x, we do not use this condition in generating the final images. This condition is equivalent to imposing a smoothness constraint on the first derivative of the image and because the Fourier transform is symmetric this prior imposes what is often referred to as a circular boundary condition.

If we assign the likelihood using a Gaussian, the joint posterior probability for τ_x, Eq. (22.9), is given by:

$$P(\tau_x|DI) \propto \int \frac{d\sigma}{\sigma} \prod_{j=1}^{N_y} \int d\theta_j dB_{1j} \ldots dB_{N_x j} \sigma^{-3N_x} \exp\left\{-\frac{Q_j}{2\sigma^2}\right\} \tag{22.13}$$

where we have dropped some constants that cancel when this distribution is normalized. The quantity Q_j is given by

$$Q_j \equiv \sum_{k=1}^{N_x}\sum_{l=1}^{N_x} B_{lj}\beta^2 U_{kl} B_{kj} + \sum_{i=1}^{N_x}\left(d_{Rij} - \sum_{k=1}^{N_x} B_{kj} M_{Rki}\right)^2 + \left(d_{Iij} + \sum_{k=1}^{N_x} B_{kj} M_{Iki}\right)^2 \tag{22.14}$$

and, up to the term from the prior probability for the amplitudes, is Chi-squared evaluated for each of the k-space data sets. If we substitute the definitions of M_{Rki} and M_{Iki}, Eqs. (22.5 and 22.6) respectively then we obtain:

$$Q_j \equiv N_x \overline{d_{xj}^2} - 2\sum_{i=1} B_{ij}[\cos\theta F_{Rij} + \sin\theta F_{Iij}] + \sum_{k=1}^{N_x}\sum_{l=1}^{N_x} B_{kj} B_{lj} V_{klj} \tag{22.15}$$

with

$$V_{klj} \equiv N_x \delta_{kl} + \beta^2 U_{kl}, \tag{22.16}$$

where δ_{kl} is a delta function,

$$\overline{d_{xj}^2} \equiv \frac{1}{N_x}\sum_{i=1}^{N_x} d_{ij}^2 \tag{22.17}$$

is the mean-square data value in the jth k-space acquisition. The projections of the data onto the model,

$$F_{Rij} \equiv \sum_{i=1}^{N_x} d_{Rij}\cos(2\pi x_k[t_{xi} + \tau_x]) - d_{Iij}\sin(2\pi x_k[t_{xi} + \tau_x]) \tag{22.18}$$

and

$$F_{Iij} \equiv \sum_{i=1}^{N_x} d_{Rij}\sin(2\pi x_k[t_{xi} + \tau_x]) + d_{Iij}\cos(2\pi x_k[t_{xi} + \tau_x]), \tag{22.19}$$

are essentially the real and imaginary parts of a time shifted discrete Fourier transform. While we have not separated the time delays from the other parts of the Fourier transform, a simple trigonometric identity will reduce these quantities to linear combinations of the real and imaginary parts of the discrete Fourier transform.

The functional from of Q_j is a quadratic in the B_{kj}, so the integrals over the B_{kj} are Gaussian quadrature integrals. Such integrals are easily evaluated and we only give the results here, one obtains

$$P(\tau_x|DI) \propto \int \frac{d\sigma}{\sigma} \prod_{j=1}^{N_y} |V_{klj}|^{-\frac{1}{2}} \int d\theta_j \sigma^{-2N_x} \exp\left\{-\frac{N_x\overline{d_{xj}^2} - \sum_{i=1}^{N_x}\hat{B}_{ij}T_{ij}}{2\sigma^2}\right\} \tag{22.20}$$

where

$$T_{ij} \equiv \cos\theta F_{Rij} + \sin\theta F_{Iij} \tag{22.21}$$

and

$$\hat{B}_{ij} = \cos\theta \hat{a}_{ij} + \sin\theta \hat{b}_{ij} \tag{22.22}$$

with

$$\hat{a}_{ij} = V_{ikj}^{-1} F_{Rkj} \quad \text{and} \quad \hat{b}_{ij} = V_{ikj}^{-1} F_{Ikj}. \tag{22.23}$$

The quantities $\hat{a}_{ij}$ and $\hat{b}_{ij}$ are essentially the real and imaginary parts of the discrete Fourier transform, while $\hat{B}_{ij}$ is the expected amplitude of the signal in the phased image.

The integral over the phase is tedious and not very illuminating, and we only sketch how this integral is evaluated. One begins by taking the sufficient statistic, the sum in Eq. (22.20), and substitutes the definitions of T_{ij} and $\hat{B}_{ij}$. This results in a quadratic expression in $\cos\theta$ and $\sin\theta$. These quadratics are then reduced to $\sin(2\theta)$ and $\cos(2\theta)$ using trigonometric identities. The resulting expression may then be rewritten in terms of $\cos(2\theta + \psi)$, where ψ is a phase. In this form the integral is of the form $\exp\{\cos(\phi)\}$ which is the integral representation of the I_o Bessel function, one obtains

$$P(\tau_x|DI) \propto \int \frac{d\sigma}{\sigma} \prod_{j=1}^{N_y} |V_{klj}|^{-\frac{1}{2}} \sigma^{-2N_x} \exp\left\{-\frac{N_x \overline{d_{xj}^2} - \frac{1}{2}\sum_{i=1}^{N_x}(\hat{a}_{ij}F_{Rij} + \hat{b}_{ij}F_{Iij})}{2\sigma^2}\right\} I_0\left(\frac{\sqrt{W_j^2 + X_j^2}}{2\sigma^2}\right) \tag{22.24}$$

with

$$W_j = \sum_{i=1}^{N_x} \frac{\hat{a}_{ij}F_{Rij} - \hat{b}_{ij}F_{Iij}}{2} \tag{22.25}$$

and

$$X_j = \sum_{i=1}^{N_x} \frac{\hat{a}_{ij}F_{Iij} + \hat{b}_{ij}F_{Rij}}{2}. \tag{22.26}$$

We note in passing that the quantity

$$\psi_j = -\frac{1}{2}\tan^{-1}\left(\frac{X_j}{W_j}\right) \tag{22.27}$$

is the estimated constant part of the phase for each of the k-space acquisitions. We mention this because in the full calculation, a quantity almost identical to this will appear as the estimated constant phase for the entire data set.

In this form the integral over the standard deviation of the noise prior probability, σ, is not easily represented in closed form. Fortunately, there is a simple easy approximation that is good to many decimal places around the maximum in Eq.(22.24). For large argument the I_0 Bessel function is nearly exponential, then Eq.(22.24) is very nearly equal to

$$P(\tau_x|DI) \approx \int \frac{d\sigma}{\sigma} \prod_{j=1}^{N_y} |V_{klj}|^{-\frac{1}{2}} \sigma^{-2N_x} \exp\left\{-\frac{N_x \overline{d_{xj}^2} - \frac{1}{2}\sum_{i=1}^{N_x}(\hat{a}_{ij}F_{Rij} + \hat{b}_{ij}F_{Iij}) - \sqrt{W_j^2 + X_j^2}}{2\sigma^2}\right\} \tag{22.28}$$

and the integral over the standard deviation may be transformed into a gamma function and we omit the details of evaluating this integral, one obtains

$$P(\tau_x|DI) \propto \prod_{j=1}^{N_y} |V_{klj}|^{-\frac{1}{2}} \left[N_x \overline{d_{xj}^2} - \frac{1}{2}\sum_{i=1}^{N_x}(\hat{a}_{ij}F_{Rij} + \hat{b}_{ij}F_{Iij}) - \sqrt{W_j^2 + X_j^2} \right]^{-N_x}. \quad (22.29)$$

This probability density function is of the form of Students t-distribution, and it is this t-distribution that is computed in the phasing algorithm.

In addition to estimating τ_x one also needs to compute the posterior probability for τ_y. However, all one needs to do is to exchange the role of x and y and in the above equations to obtain $P(\tau_y|DI)$. Consequently, we do not give this calculation. Finally, one needs to compute the posterior probability for $P(\theta|DI)$, but we already noted that the calculation is essentially identical to Eq. (22.27). Indeed all that needs to be done is to replace the sums over x by a sum over x and y and then Eq. (22.27) will give the expected value of the phase.

So here is how the calculation is actually implemented. One first computes the fast discrete Fourier transform and uses these projections to compute posterior probability for τ_x on a coarse grid. In dimensionless units τ_x varies from $N_x/4 \leq \tau_x \leq 3N_x/4$. Outside this range the posterior probability is aliased and no additional information is available. After finding the location of the peak on this coarse grid, the algorithm does a binary search for the maximum posterior probability estimate of τ_x. Then using the estimated value of τ_x the positionally dependent phase is unwrapped in the x domain. This calculation is then repeated in the y domain and the phase is again unwrapped. The constant phase is then computed. However, there is an ambiguity in the constant phase. If the calculated value of the constant phase is Θ, then the phase that gives positive amplitudes could be Θ or $\Theta + 180°$. Before setting the constant phase the program does a quick calculation to determine which phase is appropriate and finally the constant part of the phase is unwrapped. After all of the phases have been set, the program outputs the phased images as PDF files. These PDF files are what are displayed in VNMR.

22.2 Using The Package

To use the phasing package begin by loading an image. This may be done using the Vnmr files menu or you may use the **Load An Image** on the window, see Fig. 22.2. In VnmrJ the corresponding function is done on the housekeeping folder using the CWD file menu. When an image is loaded under Vnmr, the macros test to see if the image has been previously analyzed. If it has and the current setting of the parameters are the same as when the images were phase the run indicator is turned on and the package is set run. You may rerun the images at any time but assuming the previous settings of the variables are OK, there is no need to do this.

After loading an image, specify whether the image is a spin echo or EPI image. This is done using the **Image Type** menu. Here the term spin echo means only that the image may be phased using three phase parameters, so gradient echo images should be selected as spin echo. While EPI means that 4 phase parameters are needed to phase an image: the constant phase, τ_y and an even and odd delay, τ_{ex} and τ_{ox}, in x.

Next indicate how the images are to be processed using the **process** menu. The choices are All, Common or One, where "All" means that each image is to be phased using parameters specific to that image. "Common" means that phase parameters are to be computed from the currently

Figure 22.3: Linear Phasing Package The Console Log

Array	Slice	Delay X	Delay Y	Phase
33	1	66.37122551	47.85130018	285.95947785
1	1	66.18384758	47.96787733	308.70159650
34	1	66.20887199	47.97886366	304.08678779
2	1	66.20948234	47.96055311	306.64428485
35	1	66.35840813	47.91508192	292.95579385
3	1	66.21192375	47.97764295	306.10371565
36	1	66.26502434	47.90165418	294.32695098
4	1	66.23938957	47.95567030	305.71194166
37	1	66.24671379	48.01442248	302.01416187
5	1	66.29920402	47.96909803	302.93402804
38	1	66.24671379	47.94590467	300.11338126
6	1	66.26075188	47.96177381	303.08474711
39	1	66.34314934	48.01747424	299.16341694
7	1	66.20398918	47.96299451	303.84929962
40	1	66.30774895	47.87754530	292.07343083
8	1	66.20765129	47.97398084	304.35076867
41	1	66.43714348	47.64805311	266.41805910
9	1	66.20368400	47.96421522	305.24927395
42	1	66.44019523	47.96787733	292.28161251

Figure 22.3: The Phasing routine does write the value of the phase parameter to the mcmc.values file. The exact format of this file varies somewhat between spin echo images and EPI, EPI images have a fourth column: the even and odd τ_x value.

displayed image and then those phase parameters are to be applied to every image. Finally, "One" means to compute the phase parameters for the currently displayed image.

There are a number of widgets on the interface that are used to control the display and used to set the image sizes. The entry boxes labeled "fn" and "fn1" are used to enter the sizes of the Fourier transforms. If these sizes differ from the "np" and 2 times "nv" the program does the calculations using "np" and "nv" sizes and then computes and phases the final images at the "fn" and "fn1" values.

Finally, the entry boxes **cf**, **Display Array Element** and **Display** many be used to control which image is being displayed. In all cases if the phasing algorithm has been run, then the phased image is displayed, otherwise the image is displayed in absolute value mode. Changing "cf" will cause different slices to be displayed. Similarly, changing "Display Array Element" will display an image from the new array element. Finally, changing "Display" from Real to Imaginary will cause the imaginary part of the image to be displayed. Note this last widget does nothing if the phase algorithm has not be run.

The phasing routine does write the phases to the "mcmc.values" file located in the BayesOtherAnalysis directory in the current experiment. An example of this file is shown in Fig. 22.3 The phasing algorithm does use multiple threads, but not to the extent that most other algorithms do. In the case of the phasing algorithm if multiple images are to be phased each image is dispatched to a separate thread to run. This is indicated in the output list because th order of the “array” index is mixed up. This output is simply written as each thread completes phasing an image, so the order can get mixed up. Note that in the case of the image processed to produce this figure the delay in both x and y was very stable, while the constant phase did vary a little. However, even with this variation it would have been possible to phase this image using a single common set of phase parameters.

Bibliography

[1] Rev. Thomas Bayes (1763), "An Essay Toward Solving a Problem in the Doctrine of Chances," *Philos. Trans. R. Soc. London*, **53,** pp. 370-418; reprinted in *Biometrika*, **45**, pp. 293-315 (1958), and *Facsimiles of Two Papers by Bayes,* with commentary by W. Edwards Deming, New York, Hafner, 1963.

[2] G. Larry Bretthorst (1988), "Bayesian Spectrum Analysis and Parameter Estimation," in *Lecture Notes in Statistics,* **48**, J. Berger, S. Fienberg, J. Gani, K. Krickenberg, and B. Singer (eds), Springer-Verlag, New York, New York.

[3] G. Larry Bretthorst (1990), "An Introduction to Parameter Estimation Using Bayesian Probability Theory," in *Maximum Entropy and Bayesian Methods,* Dartmouth College 1989, P. Fougère *ed.,* pp. 53-79, Kluwer Academic Publishers, Dordrecht the Netherlands.

[4] G. Larry Bretthorst (1990), "Bayesian Analysis I. Parameter Estimation Using Quadrature NMR Models" *J. Magn. Reson.*, **88**, pp. 533-551.

[5] G. Larry Bretthorst (1990), "Bayesian Analysis II. Signal Detection And Model Selection" *J. Magn. Reson.*, **88**, pp. 552-570.

[6] G. Larry Bretthorst (1990), "Bayesian Analysis III. Examples Relevant to NMR" *J. Magn. Reson.*, **88**, pp. 571-595.

[7] G. Larry Bretthorst (1991), "Bayesian Analysis. IV. Noise and Computing Time Considerations," *J. Magn. Reson.*, **93**, pp. 369-394.

[8] G. Larry Bretthorst (1992), "Bayesian Analysis. V. Amplitude Estimation for Multiple Well-Separated Sinusoids," *J. Magn. Reson.*, **98**, pp. 501-523.

[9] G. Larry Bretthorst (1992), "Estimating The Ratio Of Two Amplitudes In Nuclear Magnetic Resonance Data," in *Maximum Entropy and Bayesian Methods,* C. R. Smith *et al.* (eds.), pp. 67-77, Kluwer Academic Publishers, the Netherlands.

[10] G. Larry Bretthorst (1993), "On The Difference In Means," in Physics & Probability Essays in honor of Edwin T. Jaynes, W. T. Grandy and P. W. Milonni (eds.), pp. 177-194, Cambridge University Press, England.

[11] G. Larry Bretthorst (1996), "An Introduction To Model Selection Using Bayesian Probability Theory," in *Maximum Entropy and Bayesian Methods*, G. R. Heidbreder, ed., pp. 1-42, Kluwer Academic Publishers, Printed in the Netherlands.

[12] G. Larry Bretthorst (1999), "The Near-Irrelevance of Sampling Frequency Distributions," in *Maximum Entropy and Bayesian Methods,* W. von der Linden *et al.* (eds.), pp. 21-46, Kluwer Academic Publishers, the Netherlands.

[13] G. Larry Bretthorst (2001), "Nonuniform Sampling: Bandwidth and Aliasing," in *Maximum Entropy and Bayesian Methods in Science and Engineering,* Joshua Rychert, Gary Erickson and C. Ray Smith *eds.*, pp. 1-28, American Institute of Physics, USA.

[14] G. Larry Bretthorst, Christopher D. Kroenke, and Jeffrey J. Neil (2004), "Characterizing Water Diffusion In Fixed Baboon Brain," in Bayesian Inference And Maximum Entropy Methods In Science And Engineering, Rainer Fischer, Roland Preuss and Udo von Toussaint *eds.*, AIP conference Proceedings, **735**, pp. 3-15.

[15] G. Larry Bretthorst, William C. Hutton, Joel R. Garbow, and Joseph J.H. Ackerman (2005), "Exponential parameter estimation (in NMR) using Bayesian probability theory," *Concepts in Magnetic Resonance*, 27A, Issue 2, pp. 55-63.

[16] G. Larry Bretthorst, William C. Hutton, Joel R. Garbow, and Joseph J. H. Ackerman (2005), "Exponential model selection (in NMR) using Bayesian probability theory," *Concepts in Magnetic Resonance*, 27A, Issue 2, pp. 64-72.

[17] G. Larry Bretthorst, William C. Hutton, Joel R. Garbow, and Joseph J.H. Ackerman (2005), "How accurately can parameters from exponential models be estimated? A Bayesian view," *Concepts in Magnetic Resonance*, 27A, Issue 2, pp. 73-83.

[18] G. Larry Bretthorst, W. C. Hutton, J. R. Garbow, and Joseph J. H. Ackerman (2008), "High Dynamic Range MRS Time-Domain Signal Analysis," *Magn. Reson. in Med.*, **62**, pp. 1026-1035.

[19] V. Chandramouli, K. Ekberg, W. C. Schumann, S. C. Kalhan, J. Wahren, and B. R. Landau (1997), "Quantifying gluconeogenesis during fasting," *American Journal of Physiology*, **273**, pp. H1209-H1215.

[20] R. T. Cox (1961), "The Algebra of Probable Inference," Johns Hopkins Univ. Press, Baltimore.

[21] André d'Avignon, G. Larry Bretthorst, Marlyn Emerson Holtzer, and Alfred Holtzer (1998), "Site-Specific Thermodynamics and Kinetics of a Coiled-Coil Transition by Spin Inversion Transfer NMR," *Biophysical Journal*, **74**, pp. 3190-3197.

[22] André d'Avignon, G. Larry Bretthorst, Marlyn Emerson Holtzer, and Alfred Holtzer (1999), "Thermodynamics and Kinetics of a Folded-Folded Transition at Valine-9 of a GCN4-Like Leucine Zipper," *Biophysical Journal*, **76**, pp. 2752-2759.

[23] David Freedman, and Persi Diaconis (1981), "On the histogram as a density estimator: L_2 theory," *Zeitschrift f¨r Wahrscheinlichkeitstheorie und verwandte Gebiete*, **57**, 4, pp. 453-476.

[24] W. R. Gilks, S. Richardson, and D. J. Spiegelhalter (1996), "Markov Chain Monte Carlo in Practice," Chapman & Hall, London.

[25] Paul M. Goggans, and Ying Chi (2004), "Using Thermodynamic Integration to Calculate the Posterior Probability in Bayesian Model Selection Problems," in *Bayesian Inference and Maximum Entropy Methods in Science and Engineering: 23rd International Workshop*, **707**, pp. 59-66.

[26] Marlyn Emerson Holtzer, G. Larry Bretthorst, D. André d'Avignon, Ruth Hogue Angelette, Lisa Mints, and Alfred Holtzer (2001), "Temperature Dependence of the Folding and Unfolding Kinetics of the GCN4 Leucine Lipper via 13C alpha-NMR," *Biophysical Journal*, **80**, pp. 939-951.

[27] E. T. Jaynes (1968), "Prior Probabilities," *IEEE Transactions on Systems Science and Cybernetics*, SSC-4, pp. 227-241; reprinted in [30].

[28] E. T. Jaynes (1978), "Where Do We Stand On Maximum Entropy?" in *The Maximum Entropy Formalism*, R. D. Levine and M. Tribus *Eds.*, pp. 15-118, Cambridge: MIT Press, Reprinted in [30].

[29] E. T. Jaynes (1980), "Marginalization and Prior Probabilities," in *Bayesian Analysis in Econometrics and Statistics*, A. Zellner *ed.,* North-Holland Publishing Company, Amsterdam; reprinted in [30].

[30] E. T. Jaynes (1983), "Papers on Probability, Statistics and Statistical Physics," a reprint collection, D. Reidel, Dordrecht the Netherlands; second edition Kluwer Academic Publishers, Dordrecht the Netherlands, 1989.

[31] E. T. Jaynes (1957), "How Does the Brain do Plausible Reasoning?" unpublished Stanford University Microwave Laboratory Report No. 421; reprinted in *Maximum-Entropy and Bayesian Methods in Science and Engineering* **1,** pp. 1-24, G. J. Erickson and C. R. Smith *Eds.,* 1988.

[32] E. T. Jaynes (2003), "Probability Theory—The Logic of Science," edited by G. Larry Bretthorst, Cambridge University Press, Cambridge UK.

[33] Sir Harold Jeffreys (1939), "Theory of Probability," Oxford Univ. Press, London; Later editions, 1948, 1961.

[34] John G. Jones, Michael A. Solomon, Suzanne M. Cole, A. Dean Sherry, and Craig R. Malloy (2001) "An integrated ^{2}H and ^{13}C NMR study of gluconeogenesis and TCA cycle flux in humans," *American Journal of Physiology, Endocrinology, and Metabolism,* **281,** pp. H848-H856.

[35] John Kotyk, N. G. Hoffman, W. C. Hutton, G. Larry Bretthorst, and J. J. H. Ackerman (1992), "Comparison of Fourier and Bayesian Analysis of NMR Signals. I. Well-Separated Resonances (The Single-Frequency Case)," *J. Magn. Reson.*, **98**, pp. 483–500.

[36] Pierre Simon Laplace (1814), "A Philosophical Essay on Probabilities," John Wiley & Sons, London, Chapman & Hall, Limited 1902. Translated from the 6th edition by F. W. Truscott and F. L. Emory.

[37] N. Lartillot, and H. Philippe (2006), "Computing Bayes Factors Using Thermodynamic Integration," *Systematic Biology*, **55** (2), pp. 195-207.

[38] D. Le Bihan, and E. Breton (1985), "Imagerie de diffusion in-vivo par rsonance," Comptes rendus de l'Acadmie des Sciences (Paris), **301** (15), pp. 1109-1112.

[39] N. R. Lomb (1976), "Least-Squares Frequency Analysis of Unevenly Spaced Data," *Astrophysical and Space Science*, **39**, pp. 447-462.

[40] T. J. Loredo (1990), "From Laplace To SN 1987A: Bayesian Inference In Astrophysics," in *Maximum Entropy and Bayesian Methods,* P. F. Fougere (ed), Kluwer Academic Publishers, Dordrecht, The Netherlands.

[41] Craig R. Malloy, A. Dean Sherry, and Mark Jeffrey (1988), "Evaluation of Carbon Flux and Substrate Selection through Alternate Pathways Involving the Citric Acid Cycle of the Heart by 13C NMR Spectroscopy," *Journal of Biological Chemistry*, **263** (15), pp. 6964-6971.

[42] Craig R. Malloy, Dean Sherry, and Mark Jeffrey (1990), "Analysis of tricarboxylic acid cycle of the heart using ^{13}C isotope isomers," *American Journal of Physiology*, **259**, pp. H987-H995.

[43] Lawrence R. Mead and Nikos Papanicolaou, "Maximum entropy in the problem of moments," *J. Math. Phys.* **25**, 2404–2417 (1984).

[44] K. Merboldt, Wolfgang Hanicke, and Jens Frahm (1969), "Self-diffusion NMR imaging using stimulated echoes," Journal of Magnetic Resonance, **64** (3), pp. 479-486.

[45] Nicholas Metropolis, Arianna W. Rosenbluth, Marshall N. Rosenbluth, Augusta H. Teller, and Edward Teller (1953), "Equation of State Calculations by Fast Computing Machines," Journal of Chemical Physics. The previous link is to the Americain Institute of Physics and if you do not have access to Science Sitations you many not be able to retrieve this paper.

[46] Radford M. Neal (1993), "Probabilistic Inference Using Markov Chain Monte Carlo Methods," technical report CRG-TR-93-1, Dept. of Computer Science, University of Toronto.

[47] Jeffrey J. Neil, and G. Larry Bretthorst (1993), "On the Use of Bayesian Probability Theory for Analysis of Exponential Decay Data: An Example Taken from Intravoxel Incoherent Motion Experiments," *Magn. Reson. in Med.*, **29**, pp. 642–647.

[48] H. Nyquist (1924), "Certain Factors Affecting Telegraph Speed," *Bell System Technical Journal*, **3**, pp. 324-346.

[49] H. Nyquist (1928), "Certain Topics in Telegraph Transmission Theory," *Transactions AIEE*, **3**, pp. 617-644.

[50] William H. Press, Saul A. Teukolsky, William T. Vetterling and Brian P. Flannery (1992), "Numerical Recipes The Art of Scientific Computing Second Edition," Cambridge University Press, Cambridge UK.

[51] Emanuel Parzen (1962), "On Estimation of a Probability Density Function and Mode," *Annals of Mathematical Statistics* **33**, 1065–1076

[52] Karl Pearson (1895), "Contributions to the Mathematical Theory of Evolution. II. Skew Variation in Homogeneous Material," *Phil. Trans. R. Soc. A* **186**, 343–326.

[53] Murray Rosenblatt, "Remarks on Some Nonparametric Estimates of a Density Function," *Annals of Mathematical Statistics* **27**, 832–837 (1956).

[54] Jeffery D. Scargle (1981), "Studies in Astronomical Time Series Analysis I. Random Process In The Time Domain," *Astrophysical Journal Supplement Series*, **45**, pp. 1-71.

[55] Jeffery D. Scargle (1982), "Studies in Astronomical Time Series Analysis II. Statistical Aspects of Spectral Analysis of Unevenly Sampled Data," *Astrophysical Journal*, **263**, pp. 835-853.

[56] Jeffery D. Scargle (1989), "Studies in Astronomical Time Series Analysis. III. Fourier Transforms, Autocorrelation Functions, and Cross-correlation Functions of Unevenly Spaced Data," *Astrophysical Journal*, **343**, pp. 874-887.

[57] Arthur Schuster (1905), "The Periodogram and its Optical Analogy," *Proceedings of the Royal Society of London*, **77**, p. 136-140.

[58] Claude E. Shannon (1948), "A Mathematical Theory of Communication," *Bell Syst. Tech. J.*, **27**, pp. 379-423.

[59] John E. Shore, and Rodney W. Johnson (1981), "Properties of cross-entropy minimization," *IEEE Trans. on Information Theory*, **IT-27,** No. 4, pp. 472-482.

[60] John E. Shore and Rodney W. Johnson (1980), "Axiomatic derivation of the principle of maximum entropy and the principle of minimum cross-entropy," *IEEE Trans. on Information Theory*, **IT-26** (1), pp. 26-37.

[61] Devinderjit Sivia, and John Skilling (2006), "Data Analysis: A Bayesian Tutorial," Oxford University Press, USA.

[62] Edward O. Stejskal and Tanner, J. E. (1965), "Spin Diffusion Measurements: Spin Echoes in the Presence of a Time-Dependent Field Gradient." Journal of Chemical Physics, **42** (1), pp. 288-292.

[63] D. G. Taylor and Bushell, M. C. (1985), "The spatial mapping of translational diffusion coefficients by the NMR imaging technique," Physics in Medicine and Biology, **30** (4), pp. 345-349.

[64] Myron Tribus (1969), "Rational Descriptions, Decisions and Designs," Pergamon Press, Oxford.

[65] P. M. Woodward (1953), "Probability and Information Theory, with Applications to Radar," McGraw-Hill, N. Y. Second edition (1987); R. E. Krieger Pub. Co., Malabar, Florida.

[66] Arnold Zellner (1971), "An Introduction to Bayesian Inference in Econometrics," John Wiley and Sons, New York.